Preparation and Characterization of SMA(SAN)/Silica Hybrids Derived from Water Glass

Liang Shen, Wei Zhong, Haitao Wang, Qiangguo Du, Yuliang Yang

Department of Macromolecular Science and the Key Laboratory of Molecular Engineering of Polymers, Fudan University, Shanghai 200433, China

Received 7 August 2003; accepted 27 February 2004
DOI 10.1002/app.20783
Published online in Wiley InterScience (www.interscience.wiley.com).

ABSTRACT: Poly(styrene-*co*-maleic anhydride) (SMA)/silica and poly(styrene-*co*-acrylonitrile) (SAN)/silica hybrids were prepared via a sol-gel route by using silicic acid oligomer (SAO) from water glass in this article. This convenient route is different from the traditional one from tetraethoxysilane (TEOS). The polycondensation behavior of the SAO and the aggregation behavior of the silica particles in the hybrids were investigated. The prepared SMA(SAN)/silica hybrids were characterized by infrared spectroscopy, dynamic light scattering, thermogravimetric analysis, differential scanning calorimetry, and scanning electron microscopy. The results showed that the particle size of silica in hybrids increased with increasing silica loading and decreased dramatically by adding the coupling agents. The decomposition temperature and the glass-transition temperature of the hybrids were higher than the precursory polymers. The mechanical properties of blends of acrylonitrile-butadiene-styrene copolymers (ABS) resin with the hybrids were also tested and the results indicated that the well-dispersed silica particles in the hybrids indeed reinforced the blends. Some nanocomposites based on ABS were prepared in this way. © 2004 Wiley Periodicals, Inc. J Appl Polym Sci 93: 2289–2296, 2004

Key words: nanocomposites; silicas; dynamic light scattering; mechanical properties; thermal properties

INTRODUCTION

Recently, polymer-based organic/inorganic hybrids have gained increasing attention and have been widely used in the field of material science.[1] Inorganic material such as silica exhibits excellent thermal stability and higher hardness. The incorporation of well-dispersed (preferably on the nanometer scale) silica particles into polymer matrix was proved as an extremely effective way to improve the thermal and mechanical properties of polymers.[2–3]

An important method for obtaining organic/silica hybrids at mild conditions is to mix an organic polymer and alkoxysilane [such as tetraethoxysilane (TEOS)], followed by a sol-gel reaction involving the hydrolysis and polycondensation reaction of alkoxysilane.[4–5] In early research, a review about various nanocomposites with silica was given,[6] and it was shown that, especially in polyamide or polyimide systems, high thermal stabilities and good mechanical properties were obtained.[7–9] The microstructure of an acrylic polymer/silica nanocomposite was characterized by scanning force microscopy.[10] Poly(ethylene oxide),[11] polyurethene,[12] polymethacrylates,[13] poly(methyl methacrylate),[14–15] polyaniline,[16] polyetherimide,[17] and epoxy[18] nanocomposites with SiO_2 were prepared, and it was shown that different morphologies could be generated by varying the processing conditions.

For the sake of better distribution of the inorganic particles in polymer matrix, the coupling agents [such as (aminophenyl)trimethoxysilane (APTMS), γ-glycidyloxypropyltrimethoxysilane (GPTMS), and isocyanatopropyltrimethoxysilane (ICTMS)][19–23] were used.

The sol-gel process was used to prepare poly(styrene-*co*-maleic anhydride) (SMA)/silica and poly(styrene-*co*-acrylonitrile) (SAN)/silica hybrid materials from TEOS.[24–26] However, it was found that phase separation occurred at higher silica content and the mechanical strength of the resulting films decreased, compared to that of pure polymer. Introduction of chemical bonds between the polymer and silica by using coupling agents can improve their compatibility and improve their mechanical properties.

Another way to prepare polymer/silica hybrids is by direct incorporation of silica powders into melted polymers by mixing. However, the silica powder in nanometer size is costly, and it is difficult to disperse silica particles in polymer matrix with slight aggregation.

In this article, we present a novel sol-gel route for the preparation of SMA/silica and SAN/silica hybrids

Correspondence to: Q. Du (qgdu@fudan.edu.cn).
Contract grant sponsor: Special, Funds for Major State Basic Research Projects; contract grant number: G 1999064800.

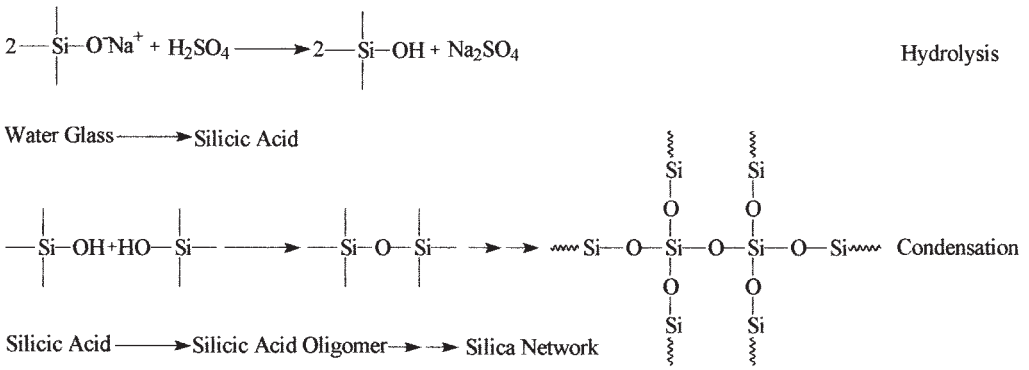

Scheme 1 The reaction process from water glass to silica network via SAO.

by using silicic acid, which was extracted from water glass, an abundant and more affordable silica precursor. The procedure from water glass to silica network via silicic acid is depicted in Scheme 1. It is expected that the hybrids can be used in the modification of acrylonitrile-butadiene-styrene copolymers (ABS) resin for their miscibility.

EXPERIMENTAL

Materials

SMA resin (MPC1555) was purchased from Shanghai Sunny New Technology Development Co. Ltd. (Shanghai, China) with maleic anhydride content of 10 wt % and melting index of 6.9 g/10 min (230°C, 2.16 kg). SAN resin (HH-C200) was provided by Lanzhou Petrochemical Co. (Lanzhou, China) with acrylonitrile content of 24.5 wt % and melting index of 2.9 g/10 min (230°C, 2.16 kg). ABS resin of high impact grade (PA-747) was purchased from Chi Mei Corp. (Tainan, Taiwan, China). Tetrahydrofuran (THF), GPTMS, and γ-aminopropyltriethoxysilane (APTES) were all analytical reagent grade, purchased from Shanghai Chemical Reagents Co. (Shanghai, China) and used without further purification. Water glass (an industrial product, the molar ratio of SiO_2 to Na_2O is 3) was purchased from Jiading Water Glass Factory (Shanghai, China) and used as received.

Preparation of the hybrids

Preparation of the solution of silicic acid in THF was as follows. A 3.2 mol/L water glass solution was adjusted to pH 2.0 with 1.0 mol/L H_2SO_4 aqueous solution under stirring at ambient conditions. This solution was saturated with sodium chloride (NaCl). Then, an equal volume of THF was added with stirring. Before the organic layer was separated, the mixture was stored at 10°C for half an hour. The silica content of the solution of silicic acid in THF was measured by thermal gravity analysis (TGA) on a Netzsch 209 instrument (Germany), assuming that all the silicic acid was transformed into silica at 700°C, the end point of the test. Preparation of the hybrids was as follows. A mixture of SMA(SAN)–THF solution, silicic acid–THF solution, and coupling agent (if needed) was stirred at room temperature for 3 h under N_2 and then cast on a polypropylene substrate. After thermal treatment at room temperature for 1 h and 90°C for 2 h in vacuum, the hybrid films were removed from the PP substrate and their thickness was around 50–100 μm.

Characterization and measurement

Fourier transform infrared spectroscopy (FTIR) spectra were recorded on a Nicolet Nexus 470 FTIR spectrophotometer (USA) with sampling suspension in potassium bromide (KBr) disk. The morphologies of the fracture surfaces of the SMA(SAN)/SiO_2 hybrids, which had been broken off in liquid nitrogen and coated with platinum, were observed with a JEOL JSM-5600LV scanning electron microscope (SEM; Japan). Dynamic light scattering (DLS) analysis of sample solutions in solvent THF was carried out on a Malvern Atousizer 4700 instrument (UK) to obtain the silica particle size and size distribution by CONTIN analysis mode. Thermal gravimetric analysis (TGA) was performed on a Netzsch 209 Thermogravimetric analyzer (Germany) at a heating rate of 10°C/min under air and temperature range from 30 to 700°C. The glass-transition temperature was measured on a Netzsch DSC 204 thermal analyzer (Germany) with a heating rate of 10°C/min under N_2 and temperature range from 30 to 250°C. The tensile properties of the blends of hybrid with ABS resin were measured on an Instron 5567 universal tester (USA) at room temperature at a drawing rate of 5 mm/min for effective sample length of 30 mm.

RESULTS AND DISCUSSION

Formation of hybrid of SiO_2 and polymer

Figure 1 showed the curve of particle distribution in the SMA/silicic acid/THF solution, which was de-

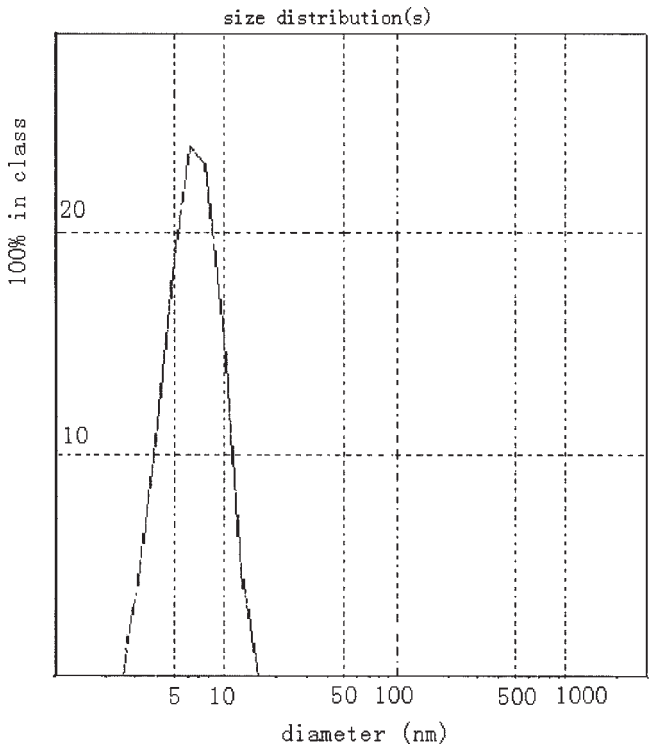

Figure 1 The size distribution of inorganic particles in SMA/silicic acid/THF.

tected by DLS. It could be seen that before the evaporation of solvent the particle size of silica network originating from silicic acid was only about 10 nm. The SEM photographs of the fracture surface of the samples obtained after evaporation of solvent and thermal treatment were shown in Figure 8(a). The well-dispersed silica particles of ~1500 nm can be clearly observed. It was during the thermal treatment when the particles of silica network aggregated to silica particles in larger size.

FTIR spectra of silica, SMA, and a sample of SMA/silica hybrid were shown in Figure 2. The characteristic absorption bands of the phenyl at 1600, 1500, 1450, and 700 cm^{-1} were observed in the FTIR spectra of the pure SMA and hybrids. The spectra also showed the absorption bands due to the C—O bond of anhydride groups stretching at 1850 and 1775 cm^{-1}. The typical absorption bands for Si—O—Si network vibrations at 1100 and 820 cm^{-1}, which did not appear in the spectrum of SMA, can be observed in the spectra of the samples of SMA/silica hybrid, and the absorption band at 1100 cm^{-1} increased with the increase in the amount of SiO_2 in the sample. The results of FTIR indicated the formation of a hybrid of silica and SMA by using the novel sol-gel route.

The effect of silica content on the particle size

With the increasing silica concentration, the silica particles tended to collide with each other, which increased the probability of aggregation of silica particles. The results of DLS were shown in Figure 3, from which we could see that the sample with lower silica content had smaller particle size. The curve of SMA showed that the sample with 5 wt % silica had silica particle size of ~600 nm, while, when the silica content reached 30 wt %, the particle size increased to 1600 nm. Corresponding with SMA/silica hybrids, the silica particle size was about 800 nm in the sample of SAN/10 wt % silica, while the silica particle size increased to 1600 nm when the silica content in SAN reached 40 wt %.

During preparation of samples with further higher silica content, the sediment was observed in the solution before evaporation because of the aggregation of silica particles.

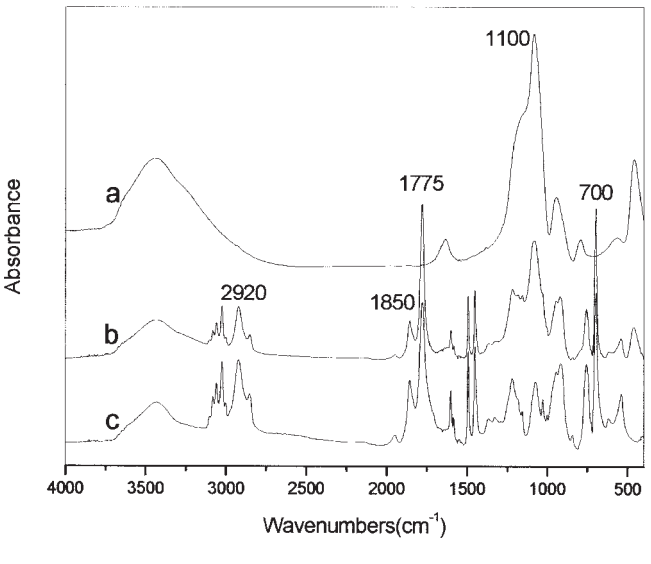

Figure 2 FTIR spectra of (a) silica, (b) SMA/20 wt % silica hybrids, and (c) virgin SMA.

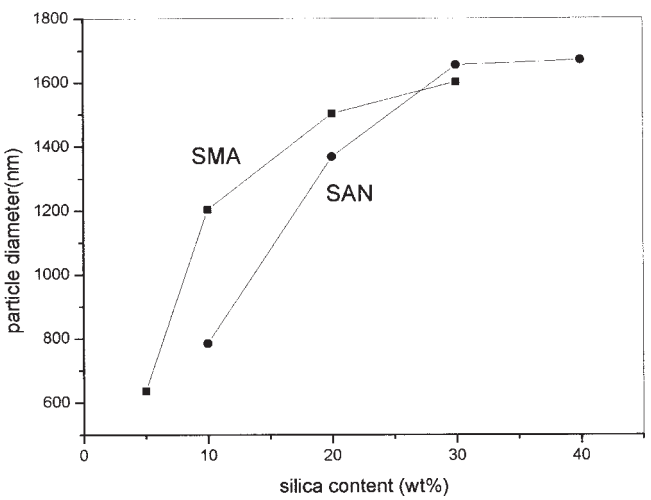

Figure 3 The average diameter of silica particles in hybrids SMA/silica and SAN/silica as a function of silica content.

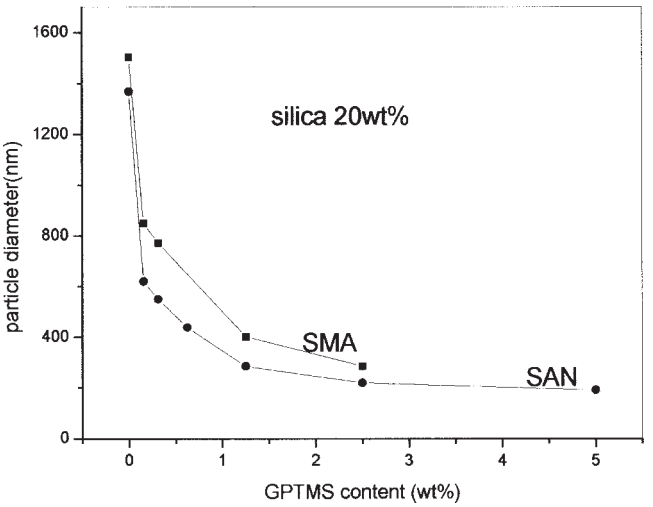

Figure 4 Effect of GPTMS on the average diameter of silica particles in SMA(SAN)/20 wt % silica hybrids.

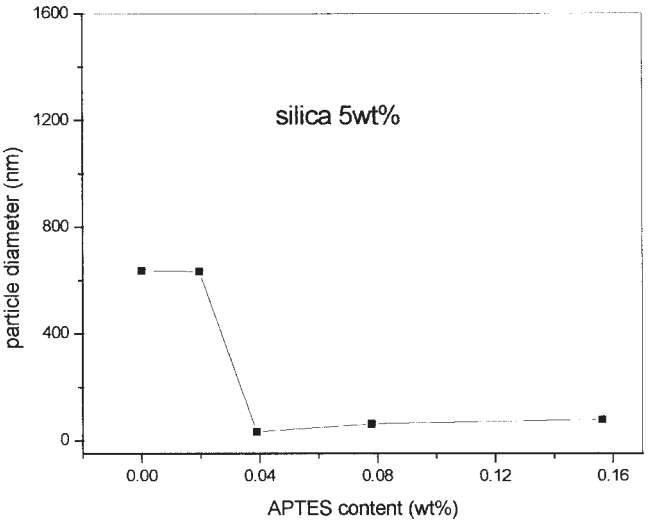

Figure 6 Effect of APTES on the average diameter of silica particles in SMA/5 wt % silica/APTES hybrids.

The effect of coupling agents on the silica particles

The size of the silica particles in hybrids could be effectively controlled by adding the coupling agents. The results measured by dynamic light scattering are shown in Figures 4–6. Both APTES and GPTMS could reduce the average size of the silica particles in the hybrids remarkably while there remained some difference between these two kinds of coupling agents. From Figure 4, it can be seen that the coupling agent GPTMS could drastically reduce the size of silica particles in both SMA/20 wt % silica and SAN/20 wt % silica hybrids with its increasing content. The effect of the coupling agent APTES on hybrids was shown in Figure 5. The size of silica particles was reduced from about 1400 to 900 nm by increasing the APTES content in SAN matrix with the silica content of 20 wt %.

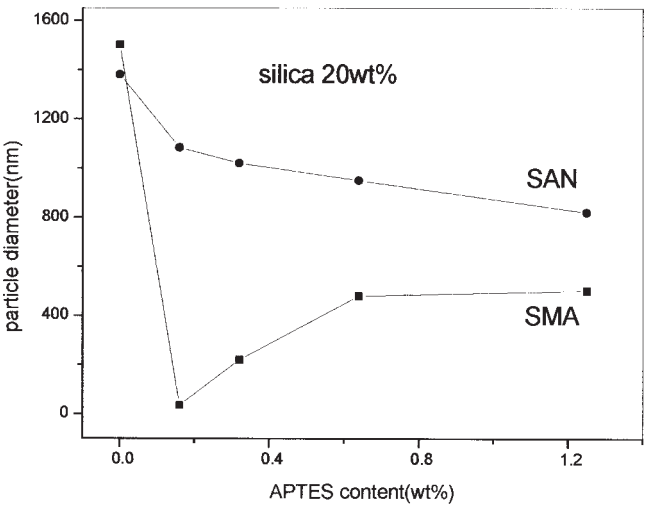

Figure 5 Effect of APTES on the average diameter of silica particles in SMA(SAN)/20 wt % silica hybrids.

However, there was some difference in SMA matrix. With the increase of APTES content, the particle size of silica first decreased from 1500 to 80 nm and then increased gradually.

It was well known that the amino groups of APTES could react with the anhydride groups of SMA, and the other end of APTES could hydrolyze to afford silanol groups that could polycondense with silicic acid oligomer (SAO; see Scheme 2). Therefore, after the coupling reaction, some covalent linkages exist between the SMA backbone and the silica network. Because of this, the aggregation of the silica particles could be effectively prevented, and a much better dispersion in SMA matrix could be achieved. On the other hand, silica particles could be bridged by SMA molecules, when APTES content increased further. Therefore, with higher APTES content, some particles in solution of the hybrid sample might consist of more than one silica particle. That was why the value of particle size measured by DLS fell first and then

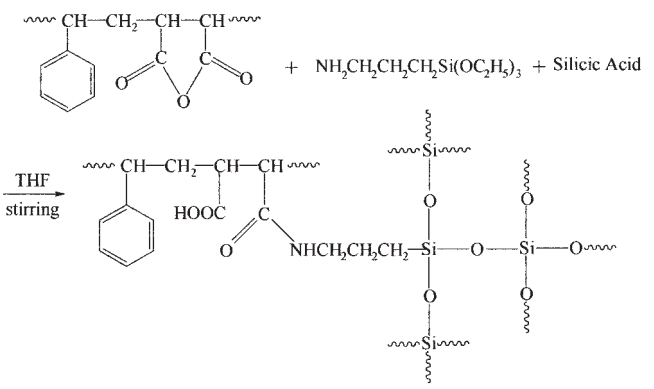

Scheme 2 The reaction of APTES with SMA and silicic acid.

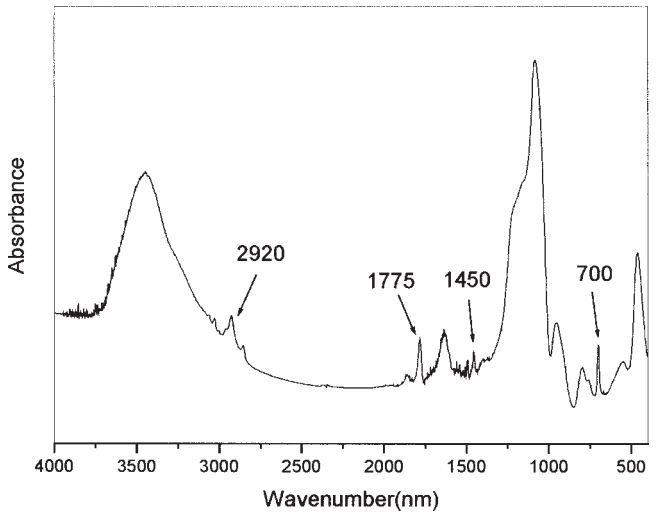

Figure 7 FTIR spectra of insoluble parts of SMA/silica/1.25 wt % APTES hybrids dissolved in THF.

climbed gradually. In fact, the hybrid sample became partly soluble in THF when content of APTES increased to 1.25 wt %. The FTIR spectrum of the insoluble part separated from the solution was shown in Figure 7, where the absorption (labeled by arrows) at 3125–2825, 1850, 1775, 1600–1400, and 700 cm^{-1} assigned to SMA could be clearly found. It proved that some silica particles were grafted and bridged by SMA through the coupling agent.

The SEM photographs of the fracture surface of the hybrid films with and without coupling agent (APTES) are shown in Figure 8. The sizes of the dispersed silica particles were about 0.8–1.6 μm (without coupling agent) and 80 nm (with 0.16 wt % of coupling agent), respectively. By comparison of these two samples, it can be seen that the silica particles in the hybrids with APTES had become much smaller in size and narrower in distribution than those in the hybrids without APTES.

The average silica particle diameter of SMA/5 wt % silica hybrids could be reduced to <100 nm with the APTES content from 0.04 to 0.16 wt %, as shown in Figure 6. It provided a way to prepare nanocomposites of silica.

The particle size also could be judged from the optical transparency of the hybrid films. The nanocomposites with smaller size of inorganic particles normally results in better transparency. As shown in Figure 9, judged by the definition of the letters under sample films (all the sample films were a consistent 100-μm thickness, which were hot-pressed at 200°C into sheets), the SMA/silica hybrids with APTES were much more transparent than the corresponding hybrids without APTES at the same thickness. The results suggested the silica particle size in sample (a) was much larger than in sample (b) and (c). Previous studies[18,27] addressed the transparent properties, which represented a signification of polymer/silica nanocomposites.

Thermal properties of SMA(SAN)/SiO_2 hybrids

TGA was used to study the thermal properties of the SMA(SAN)/silica films and the decomposition temperature is listed in Table I. TGA curves did not show weight loss <100°C, indicating no water and THF remained in the film. It was generally believed that the introduction of inorganic components into organic

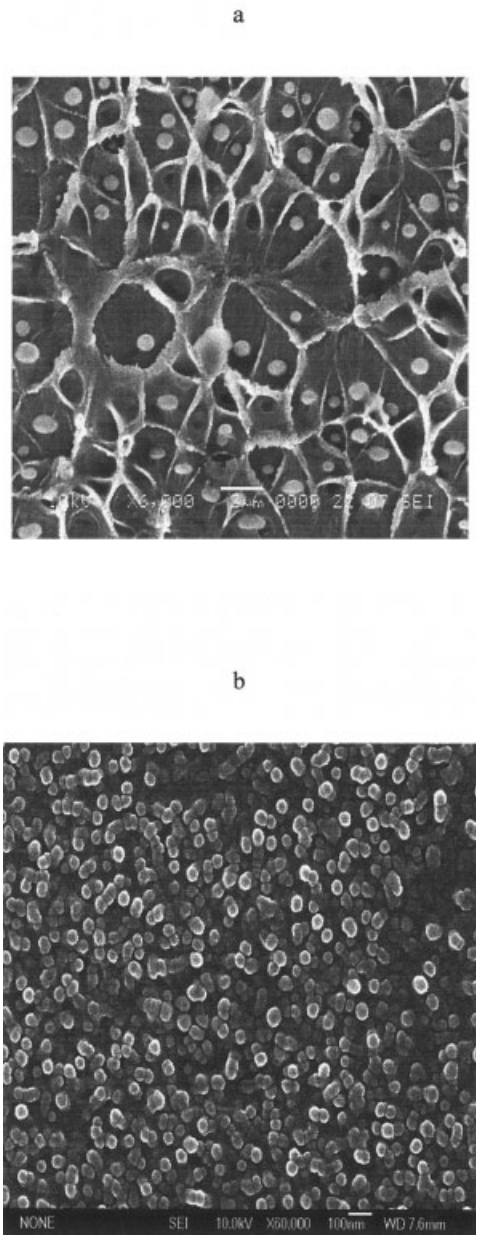

Figure 8 SEM photographs of the SMA/20 wt % SiO_2 hybrids: (a) without APTES, ×6000; (b) 0.16 wt % APTES, ×60,000.

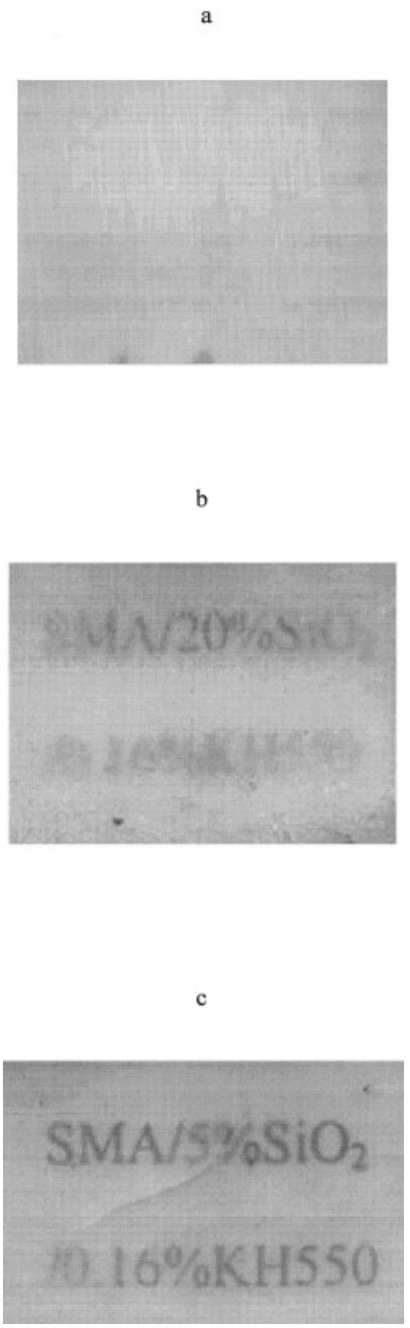

Figure 9 Pictures of printed paper covered with hybrid film of 50 μm: (a) SMA/20 wt % silica; (b) SMA/20 wt % silica/0.16 wt % APTES; (c) SMA/5 wt % silica/0.16 wt % APTES.

materials could improve their thermal stability on the basis of the fact that these species had good thermal stability. From Table I, we found that the decomposition temperature (T_d) of the hybrids was raised with the amount of the silica. The weight residue remaining at 700°C was regarded as the real silica content. As shown in Figure 10, the hybrids with coupling agents had lower initial thermal decomposition at about 150°C, similar to the pure polymers, which was perhaps due to the improved compatibility between the organic and inorganic phases.

The glass transition temperature (T_g) of the SMA(SAN)/silica hybrids increased with increasing silica content, but not remarkably. As shown in Table II, the introduction of the inorganic component increased the T_g of the SMA from 131.7 to 134.5°C and the SAN from 105.6 to 108.0°C as evidence of increased rigidity.

The connection between silica particles and SMA(SAN) molecules through coupling agent limited the chain motion of the polymers, which contributed to the elevation of T_g, whereas the flexible segments of the coupling agent limited the further enhancement of T_g. Accordingly, adding APTES in the preparation of the hybrids only can slightly raise T_g of the hybrids (see Table II).

Mechanical properties of SMA(SAN)/SiO_2 hybrids

Commonly, SAN is used as the matrix of ABS resin, and SMA is applied to blend with other polymers. SMA material used above in preparation of SMA/silica hybrids contains 10 wt % maleic anhydride, which was reported to be compatible with commercial SAN[28–30] resin or ABS resin. In this study, the hybrids were mixed with ABS resin in solution to give a series of blends containing 5 wt % silica, and the tensile properties of blend films were measured on an Instron mechanical testing machine. The values of elongation at break, tensile strength, and Young's modulus are listed in Table III. In comparison with the blends of ABS/SMA or ABS/SAN, the blend samples of ABS/hybrid containing 5 wt % silica had higher tensile intensity and Young's modulus but lower elongation at break. The reinforcement of the softer polymer due to silica particles was clearly demonstrated. By inspecting Table III, one can also find that much higher tensile intensity and Young's modulus can be obtained with blends for which the hybrid samples contained coupling agent. This is attributed to the bond-

TABLE I
Data of Decomposition Temperature of Hybrids by TGA

Matrix	Silica (wt %)	Coupling agents	Coupling agents content (wt %)	T_d (°C)[a]
SMA				393.4
SMA	5			393.8
SMA	10			394.6
SMA	15			395.4
SMA	20			397.8
SMA	5	APTES	0.04	392.1
SMA	5	APTES	0.16	391.3
SMA	20	APTES	0.16	392.4

[a] Observed from the thermogravimetric analysis at a heating rate of 10°C/min in air.

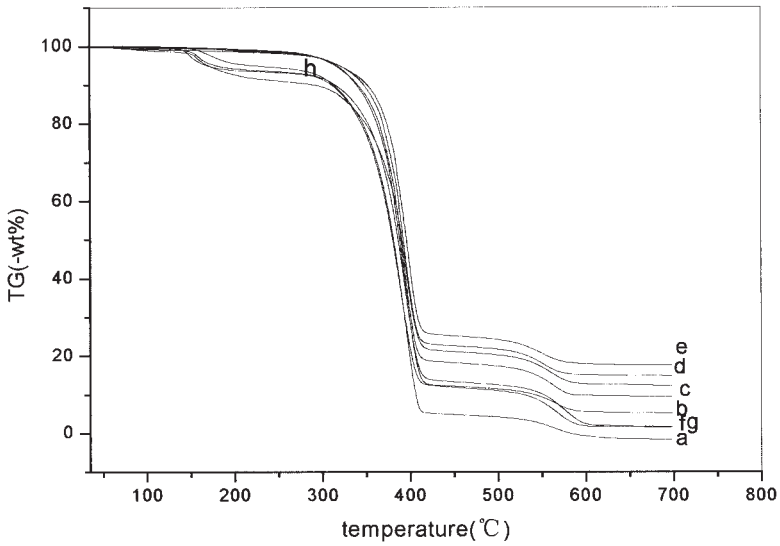

Figure 10 TGA curves of (a) SMA; (b) SMA/5 wt % SiO_2; (c) SMA/10 wt % SiO_2; (d) SMA/15 wt % SiO_2; (e) SMA/20 wt % SiO_2; (f) SMA/5 wt % SiO_2/0.04 wt % APTES; (g) SMA/5 wt % SiO_2/0.16 wt % APTES; (h) SMA/20 wt % SiO_2/0.16 wt % APTES.

ing between the silica particles and polymer. For the blend of SMA/20% silica hybrid containing 0.16 wt % APTES especially, in which silica particles were in nanometer size, a distinct increase in tensile strength and Young's modulus was observed. Because of the good compatibility between SMA (SAN) and ABS, this method is probably useful in the reinforcement of ABS resin.

In comparison with the blends of ABS/SAN, the lower tensile properties of the blends of ABS/SMA were mainly due to the brittleness of SMA.

CONCLUSION

The SMA(SAN)/SiO_2 hybrids were prepared successfully by mixing of polymer, silicic acid (from water glass), and coupling agents, followed by the sol-gel process. The polycondensation behavior of the SAO and the aggregation behavior of the silica particles mainly occurred during the thermal treatment. The good distribution and small size of silica particles in hybrids mainly resulted from the strong interaction between polymer and silica through coupling agents. The size and distribution of silica were affected by the factors as follows: (1) the content of silica, (2) the kind of coupling agent, and (3) the content of coupling agent. We can get nanocomposites when the phase separation of the organic and inorganic components is controlled in a lower level by the addition of APTES in SMA matrix. The improvement in the thermal and mechanical properties of the hybrids can be observed. This demonstrates that the well-dispersed particles of silica in the hybrid indeed reinforce these hybrid materials.

TABLE II
Data of Glass Transition Temperature of Hybrids by DSC

Matrix	Silica (wt %)	Coupling agents	Coupling agents content (wt %)	Silica particle diameter (nm)[a]	T_g (°C)[b]
SMA					131.7
SMA	5			636	133.5
SMA	5	APTES	0.04	32.4	133.0
SMA	20			1503	134.5
SMA	20	APTES	0.16	35.9	136.0
SAN					105.6
SAN	20			1368	108.0
SAN	20	APTES	0.16	1083	107.8
SAN	20	GPTMS	0.16	620	109.0

[a] Determined by DLS.
[b] Observed in the DSC measured at a heating rate of 10°C/min in nitrogen.

TABLE III
Mechanical Properties of Blends of the Hybrids with ABS

ABS/hybrid (by weight)	Hybrid				Elongation at break (%)	Tensile strength (MPa)	Young's modulus (GPa)
	Matrix	Silica in hybrid (wt %)	Type of coupling agent	Coupling agent (wt %)			
4/1	SMA	0	—	—	2.8	18.2	1.05
4/1	SMA	20	—	—	2.1	23.1	1.25
4/1	SMA	20	GPTMS	0.16	2.4	23.3	1.39
4/1	SMA	20	APTES	0.16	2.5	27.2	1.69
4/1	SAN	0	—	—	3.8	26.6	1.30
4/1	SAN	20	—	—	4.0	36.6	1.96
4/1	SAN	20	GPTMS	0.16	3.4	42.1	2.50
4/1	SAN	20	APTES	0.16	2.8	35.6	2.29

This work were subsidized by the Special Funds for Major State Basic Research Projects (G1999064800).

References

1. Breen, C.; Hay, J. Mater World 2003, 11, 30.
2. Sharp, K. G. Adv Mater. 1998, 10, 1243.
3. Zhu, Z.; Yang, Y.; Yin, J.; Qi, Z. J Appl Polym Sci 1999, 73, 2977.
4. Schmidt, H.; Jonschker, G.; Giedicke, S.; Menning, M. J Sol-Gel Sci Technol 2000, 19, 39.
5. Hench, L. L.; West, J. K. Chem Rev 1990, 90, 33.
6. Mark, J. E. in Int SAMPE Tech Conf, Vol 27: Diversity into the Next Century; Cincinnati, OH, 1995; p. 539.
7. Chen, Y.; Iroh, J. O.; Chem Mater 1999, 11, 1218.
8. Zhu, Z. K.; Yin, J.; Cao, F.; Shang, X. Y.; Lu, Q. H. Adv Mater 2000, 12, 1055.
9. van Zyl, W. E.; Garcia, M.; Schrauwen, B. A. G.; Kooi, B. J.; De Hosson, J. M.; Verweij, H. Macromol Mater Eng 2002, 287, 106.
10. Motomatsu, M.; Takahashi, T.; Nie, H-Y.; Mizutani, W.; Tokumoto, H.; Polymer 1997, 38, 177.
11. Wojcik, A. B.; Ting, A.; Klein, L. C. Mater Sci Eng 1998, C6, 115.
12. Gerard, J. F.; Kaddami, H.; Pascault, J. P. in Ext. Abstr.-EUROFILLERS 97, 2nd Int. Conf. Filled Plym. Fillers; Lyon, 1997; p. 407.
13. Wei, Y.; Feng, Q. F.; Xu, J. G.; Dong, H.; Qiu, K. Y.; Jansen, S. A.; Yin, R.; Ong, F. K. Adv Mater., 2000, 12, 1448.
14. Silveire, K. F.; Valeria, I.; Yoshida, P.; Nunes, S. P. Polymer 1995, 36, 1425.
15. Qin, H. H.; Dong, J. H.; Qiu, K. Y.; Wei, Y. J Poly Sci, Part A: Polym Chem 2000; 38, 321.
16. Wang, Y. J.; Wang, X. H.; Li, J.; Mo, Z. S.; Zhao, X. J. Jing, X. B.; Wang, F. S. Adv Mater 2001, 13, 1582.
17. Nunes, S. P.; Peinemann, K. V.; Ohlrogge, K.; Alpers, A.; Keller, M.; Pires, A. T. N. J Membrane Sci 1999, 157, 219.
18. Wang, Z.; Lan, T.; Pinnavaia, T. L. Chem Mater 1996, 8, 2200.
19. Sysel, P.; Pulec, R.; Maryska, M. Polym J. 1997, 29, 607.
20. Macia, L.; Kioul, A. J Mater Sci Lett 1994, 13, 641.
21. Kioul, A.; Mascia, L. J. Noncryst Solids 1994, 175, 169.
22. Mascia, L.; Kioul, A. Polymer 1995, 36, 3649.
23. Menoyo, J. D. C.; Mascia, L.; Shaw, S. J Mater Res Soc Symp Proc 1998, 520, 239.
24. Zhou, W.; Dong, J. H.; Qiu, S. Y.; Wei, Y. Acta Polym Sinica 1998, 6, 730.
25. Zhao, D. Z.; Ou, C. Y.; Gao, M. Z. Acta Polym Sinica 1996, 2, 228.
26. Eisenberg, P.; Lucas, J. C.; Williams, R. J. J. Macromol Symp 2002, 189, 1.
27. Shang, X. Y.; Zhu, Z. K.; Yin, J.; Ma, X. D. Chem Mater 2002, 14, 71.
28. Aoki, Y. Macromolecules 1988, 21, 1277.
29. Tacx, J. C. J. F.; Roolant, H.; Francken, R. T. G.; Reid, V. M. C. Polymer 2002, 43, 737.
30. Pathak, J. A.; van Gurp, M. J Appl Polym Sci., 2000, 78, 1245.